Optimization of EMG-Derived Features for Upper Limb Prosthetic Control

Optimization of EMG-derived features for upper limb prosthetic control

Dario Di Domenico[1,2,*] [0000−0002−4603−1692], Francesca Paganini[1,3,*] [0009−0007−1908−3554], Andrea Marinelli[1,4] [0000−0001−8672−5202], Lorenzo De Michieli[1] [0000−0001−7158−3002], Nicoló Boccardo[1,5] [0000−0002−3460−7068], and Marianna Semprini[1] [0000−0001−5504−0251]

[1] Rehab Technologies Lab, Italian Institute of Technology, Via Morego, 30, Genova 16163, Italy
[2] Department of Electronics and Telecommunications, Politecnico di Torino, Turin 10124, Italy
[3] Department of Mechanical and Process Engineering, University of Applied Science Offenburg, Offenburg 77652, Germany
[4] Bioengineering Lab, University of Genova, DIBRIS, Genova, Italy
[5] Open University Affiliated Research Centre at Istituto Italiano di Tecnologia (ARC@IIT), Genova, Italy

Abstract. Polyarticulated active prostheses constitute a promising solution for upper limb amputees. The bottleneck for their adoption though, is the lack of intuitive control. In this context, machine learning algorithms based on pattern recognition from electromyographic (EMG) signals represent a great opportunity for naturally operating prosthetic devices, but their performance is strongly affected by the selection of input features. In this study, we investigated different combinations of 13 EMG-derived features obtained from EMG signals of healthy individuals performing upper limb movements and tested their performance for movement classification using an Artificial Neural Network. We found that input data (i.e., the set of input features) can be reduced by more than 50% without any loss in accuracy, while diminishing the computing time required to train the classifier. Our results indicate that input features must be properly selected in order to optimize prosthetic control.

Keywords: EMG features · Machine Learning · Myocontrol · Prosthetic control.

1 INTRODUCTION

With the loss of a hand, the level of autonomy and ability to perform work, social, and activities of daily living (ADLs) can be significantly reduced. Prosthetic devices have evolved over time from simple mechanical and passive devices to more sophisticated mechatronic systems designed to be controlled by human

[*] These authors contributed equally to this work

intentions, often by means of electronic sensors able to detect electromyographic (EMG) activity of the residual limb [9]. Myoelectric prostheses thus translate muscle activity into information used to control the movements of the prosthetic limb. The control is proportional, meaning that the higher the EMG signal, the faster the prosthesis moves [1]. This allows the amputee to control the force and speed of movement by varying the intensity of muscle contraction.
Today, the most common upper extremity prosthetic control strategy available on the market, still relies on two muscle contractions. Since controlling multiple joints simultaneously is still a challenge, the control is generally limited to a single DoF at a time. Switching from one joint movement to another is typically accomplished through simultaneous contraction of the flexor and extensor muscles of the wrist (co-contraction) [14].

Researchers are thus investigating new techniques based on pattern recognition and machine learning algorithms to improve control strategies and make prosthetic devices more reliable and naturally activated [3]. In this scenario, EMG signal is typically processed and turned into input for the control algorithm. Current research aims at increasing the accuracy of predicting human intentions from EMG-derived features, as the number of degrees of freedom (DoFs) for prosthetic movements increases [9]. Many control algorithms have been proposed but the main problems remain accurate signal detection and fast processing (for a review, see [5]). In particular, the literature is lacking of studies addressing the choice of training method and the composition of the training dataset [5].

To address these issues, we here aim to tackle the composition of the input dataset and we study the relationship between muscle activation and generated movements during reaching and grasping tasks, by examining the key components of EMG signals and with the goal of better understanding the key biomechanical elements of upper limb movements in healthy subjects. The final goal is to determine which control algorithm inputs (i.e., *EMG-derived features*) are more appropriate to both increase the accuracy of the control algorithm and reduce the computational effort. This study could have a crucial impact for the control of upper limb prostheses.

2 MATERIALS AND METHODS

2.1 Subjects and experimental setup

Thirteen healthy participants (8 males, aged 29.7 ± 3.8 years) voluntarily took part to the experiments after having signed an informed consent. The Italian Institute of Research Ethics Committee approved the study protocol and procedures, assessing that all the requirements of the Declaration of Helsinki were followed.

Myoelectric activity was measured by recording EMG signals via high-density surface EMG with a portable 64-channels amplifier (Sessantaquattro, OT Bioelettronica, Torino, Italy) to which two 32-channels electrode grids were connected.

The two grids were attached to the forearm of the subject proximally 5cm below the olecranon. The first patch (electrodes 1-32) was placed on flexor muscles of the fingers, while the second patch (electrodes 33-64) was placed on the extensor muscles of the fingers. The position of the patches was decided in order to cover the entire circumference of the forearm. Grids were configured with 8x4 electrodes, with an inter-electrode distance of 10mm. The first grid was placed over flexor extrinsic hand muscles, in the mid of the ventral side of the forearm, while the second grid was placed over extensor extrinsic hand muscles on the dorsal side of the forearm, in the first proximal third of the forearm. Ulna palpation was used as a reference, as well as muscle palpation during prescribed contraction actuating the muscles of interest. The signal was sampled at 2000Hz and A/D converted on 24 bits.

2.2 Experimental protocol

This study is based on two datasets: one used to evaluate whether and how different EMG-derived features convey the same information about the underlying movement generated (dataset-1); and one used to test the efficacy of such combinations for prosthetic control (dataset-2).

To create dataset-1, 10 of the recruited subjects were asked to perform 16 tasks, which ranged from simple hand gestures like Hand Opening (HO) or Hand Closing (HC), Wrist Extension and Flexion (WE and WF) or Wrist Supination and Pronation (WS and WP), to more complex tasks which involved reaching and grasping of objects of different shapes (i.e., Cylindrical grasp, Spherical grasp, Tri-digital grasp, Thumb opposition, Frontal reaching, Cylindrical reaching, Spherical reaching, Pour a water glass, Screw a bottle cap, Bring an object to mouth). Each gesture was repeated 10 times and muscular activities were captured by the Sessantaquattro device (OTBioelettronica, Torino, Italy) equipped with two matrices of EMG sensors (4X8), as represented in Figure 1.

To create dataset-2, high-density EMG signals were acquired from 3 subjects while performing 10 repetition of simple hand gestures (HO, HC, WP, WS, WF, WE) and rest. The data was acquired such that for each repetition of each movement, only the transitory phase and the steady state phase of maximal contraction were included, with each repetition consisting of approximately 2s. The acquisition thus started as the subject was performing the movement and continued during the steady state. At this point, the subject was required to keep contracting the muscle until the end of the 2s of acquisition; after the acquisition was stopped the subject could relax the muscle to avoid fatigue. For each movement this process was repeated 10 times.

2.3 Signal processing and EMG-derived features extraction

For both datasets, the raw EMG signals acquired were preprocessed with a 4^{th} order Butterworth bandpass filter with a low cutoff frequency of 20Hz and a high cutoff frequency of 500Hz.

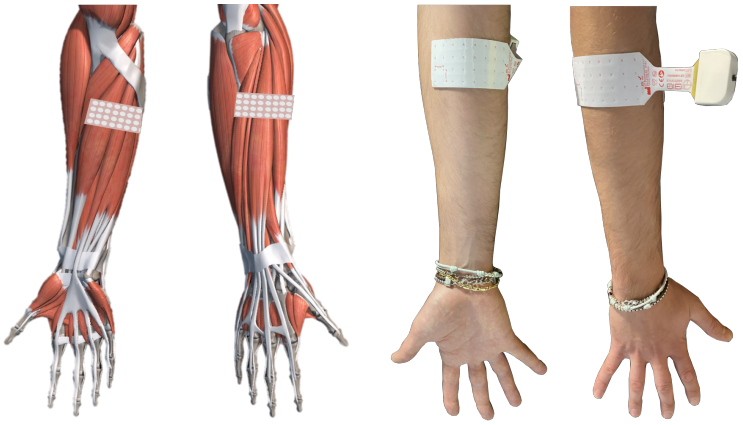

Fig. 1. Experimental setup

EMG-derived features were extracted from the preprocessed EMG signals using a sliding-window of 200ms (400 samples) with an increment of 50ms (100 samples). To allow a comparison between different conditions, the features were then normalized by subtracting the minimum value of each EMG channel and by dividing for the difference between the maximum range.

The selected EMG-derived features are the most used in prosthetic applications [8], [11] and are presented in Tab. 2. All data processing was performed using Matlab (Mathworks).

2.4 Combinations of EMG-derived features

To evaluate whether pairs of features share a similar content of information about the underlying movement, we calculated their Cross Correlation (CC). CC was calculated for each couple of features that were extracted from dataset-1, then the mean CC across all tasks and all subjects was calculated. Combinations of EMG-derived features were then calculated according to CC results as follows. First, groups of features with high correlation were identified, then different combinations were created using one or more features per group, taking into account all the possible combinations.

2.5 Evaluation of EMG-derived features combinations

Dataset-2 was used to test the performance of different combinations of EMG-derived features for movement classification, i.e., for operating a prosthetic device. To this end, features were extracted from dataset-2 and then supplied to a machine learning classifier (Artificial Neural Network: ANN [4]). For each group of hyperparameters the dataset was randomly split in training set (Tr=80%) and test set (Ts=20%). The hyperparameters of the ANN classifier were optimized using a grid search strategy [7]. In particular, the number of layers was

Table 1. Name and formula of the EMG-derived features.

	Feature name	**Formula**
1	Mean Square (MS)	$\frac{1}{N}\sum_{i=1}^{N} x_i^2$
2	Root Mean Square (RMS)	$\sqrt{\frac{1}{N}\sum_{i=1}^{N} x_i^2}$
3	Mean Absolute Value (MAV)	$\frac{1}{N}\sum_{i=1}^{N} \mid x_i \mid$
4	Difference Absolute Standard Deviation (DABS)	$\sqrt{\frac{1}{N-1}\sum_{i=2}^{N}(x_i - x_{i-1})^2}$
5	Waveform Length (WL)	$\sum_{i=1}^{N-1} \mid x_{i+1} - x_i \mid$
6	Maximum Fractal Length (MFL)	$\log(\sqrt{\sum_{i=2}^{N}(x_i - x_{i-1})^2})$
7	Zero Crossing (ZC)	$\sum_{i=2}^{N} \mathrm{sgn}(-x_{i-1}x_i)$
8	Slope Sign Change (SSC)	$\sum_{i=2}^{N} \mathrm{sgn}[-(x_i - x_{i-1})(x_{i-1} - x_{i-2})]$
9	Willison Amplitude (WA)	$\sum_{i=2}^{N} \mathrm{sgn}(\mid x_i - x_{i-1} \mid -x_{std})$
10	Myopulse Percentage Rate (MPR)	$\sum_{i=1}^{N} \mathrm{sgn}(\mid x_i \mid -x_{std})$
11	Logarithm Detector (LD)	$\exp(\frac{1}{N}\sum_{i=1}^{N} \log \mid x_i \mid)$
12	V-Order (V3)	$\sqrt[3]{\frac{1}{N}\sum_{i=1}^{N} x_i^3}$
13	Mean Absolute Value Slope (MAVS)	$\frac{\sum_{i=2}^{N/2}\mid x_i \mid - \sum_{i=N/2+1}^{N}\mid x_i \mid}{N/2}$

changed between 1 and 2. The number of neurons varied between 8 and 64 with logarithmic scale of base 2. The learning rate varied logarithmically with scale 10 between 1e-6 and 1e-3. The batch-size varied between 4 and 16 with a logarithmic scale of base 2. The aforementioned parameters were optimized for each subject on *Tr*. Moreover, Adam optimizer [6] was used to iteratively update network weights based on training data.

To evaluate the performance of the classifier on the *Ts* and measure the accuracy of predictions and computing time, the ANN was trained on *Tr* using various combinations of features as input. This process was repeated 100 times as the training process of the network is not stochastic, thus the robustness of the classifier was also tested. Such method, combined with the generalization of the neural network helped to avoid overfitting [13].

The computational effort was analyzed by measuring the required computing time at the end of each iteration. It must be underlined that it is evaluated on the basis of the time required by the code to compute the features on the whole dataset-2. Therefore, this assessment reflects the time needed to compute the same set of EMG-derived features in the application of real-time prosthetic control.

To assess statistical difference among performance obtained with different combination of features, the following steps were taken. First, data normality was tested with Kolmogorov-Smirnov test. Then, we run a one-way analysis of variance (either ANOVA or Kruskal-Wallis) using COMBINATION (i.e., com-

binations of features) as between factor, for accuracy and computing time separately. Post-hoc analysis was performed using Tukey-Kramer procedure. The significant level was set at $p = 0.05$.

3 RESULTS

3.1 Identification of optimal sets of features

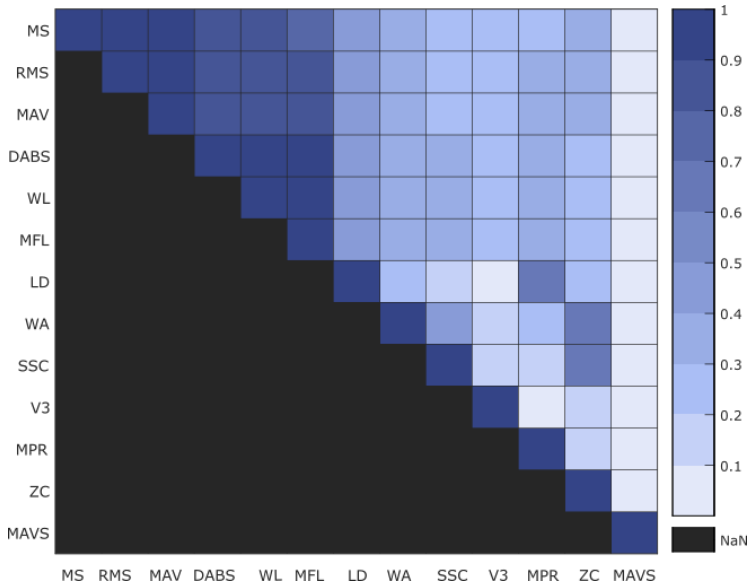

Fig. 2. Cross-correlation among pairs of EMG-derived features.

Figure 2 shows CC among pairs of features. It emerges that EMG-derived features can be grouped into 4 sets, each identified by a value of CC >60% among each couple of features. The identified groups of features are thus the following:

- Group 1: MS, RMS, MAV, DABS, WL, MFL
- Group 2: LD, MPR
- Group 3: ZC, SSC
- Group 4: ZC, WA

Following identification of redundant features, we defined different sets of them, using only one feature from each group in different possible combinations. From the first group, the RMS was identified as the best feature, since it is the most widespread in prosthetic applications [2] and it was the only feature used for its group. For groups 2-3-4 all the possible permutations were tested.

The obtained combinations are listed in Table 2, Combination-0 being the combination with all the 13 features. These combinations were then used with dataset-2 to feed the ANN classifier and evaluate both its accuracy and computing time.

Table 2. Combinations of EMG-derived features

Combination	***Features***
Combination 0	All features
Combination 1	RMS, SSC, WA, LD, V3, MAVS
Combination 2	RMS, SSC, WA, MPR, V3, MAVS
Combination 3	RMS, ZC, WA, MPR, V3, MAVS
Combination 4	RMS, ZC, WA, LD, V3, MAVS
Combination 5	RMS, ZC, SSC, WA, MPR, LD, V3, MAVS
Combination 6	RMS, ZC, MPR, V3, MAVS
Combination 7	RMS, ZC, LD, V3, MAVS
Combination 8	RMS, SSC, ZC, MPR, V3, MAVS
Combination 9	RMS, SSC, ZC, LD, V3, MAVS

3.2 Evaluation of performance of different sets of features

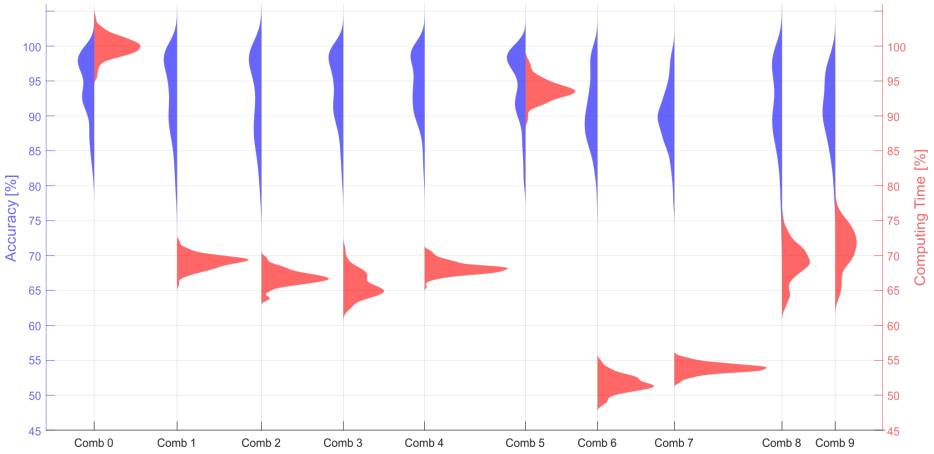

Fig. 3. Accuracy and computing time for each combination of features. The computing time is normalized relative to the mean computing time of combination-0.

Figure 3 displays accuracy and computing time for each combination of features, with the computing time being normalized relative to the mean computing time of Combination 0. Table 3 compares the accuracy and computing times of

each combination of features, reporting their median, mean and standard deviation (std).

Table 3. Median, mean and standard deviation of accuracy and computing time of each combination of features.

Combination:	0	1	2	3	4	5	6	7	8	9
Median Accuracy	94.38	93.75	93.75	94.38	94.38	95.31	90.00	89.38	90.63	90.63
Mean Accuracy	93.31	92.66	92.48	93.63	93.93	93.55	90.06	88.77	90.01	90.11
Std Accuracy	5.58	6.20	6.24	5.22	4.96	5.94	6.10	6.17	8.38	6.61
Median Computing Time	99.79	69.08	66.72	65.51	68.08	93.66	51.59	53.81	69.10	71.38
Mean Computing Time	100.00	69.93	66.67	66.06	68.76	96.34	51.83	53.66	68.79	71.08
Std Computing Time	7.08	9.19	2.34	2.82	4.84	11.36	1.81	1.47	3.25	3.07

Accuracy Figure 4 shows, for each combination of features, accuracy results across the 100 runs with each combination. Kruskal-Wallis test results indicated a significant effect of COMBINATION ($p \ll 0.05$, Bonferroni corrected) and post-hoc analysis indicated that for several pairs of combinations accuracy was not significantly different. Interestingly, we found that accuracy of combination-0 did not differ from that of combinations 3 ($p = 0.99$), 4 ($p = 0.65$) and 5 ($p = 0.94$), indicating that the same level of accuracy can be reached with a smaller number of features.

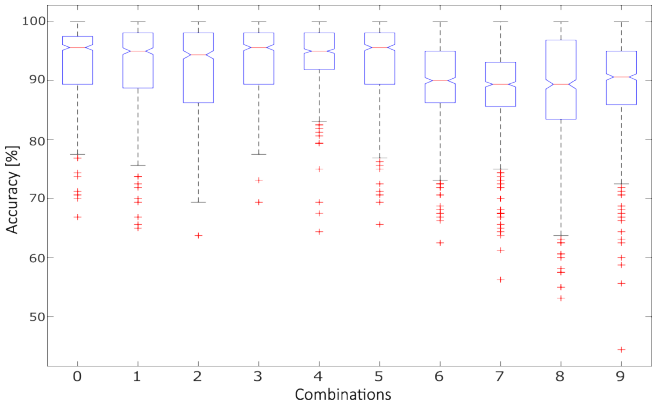

Fig. 4. Box-plots of accuracy obtained for each combination of features.

Computing Time Figure 5 shows the computing time required for each combination of features, each run 100 times. ANOVA results indicated a significant

effect of COMBINATION ($p \ll 0.05$, Bonferroni corrected) and post-hoc analysis indicated that computing time was significantly different for each pair of combinations with the exception of combination 2 and 3 and of 4 and 8. Importantly, all combinations showed a significantly smaller computation time with respect to that of combination-0 3, indicating that reducing the number of input features directly affects the computation effort.

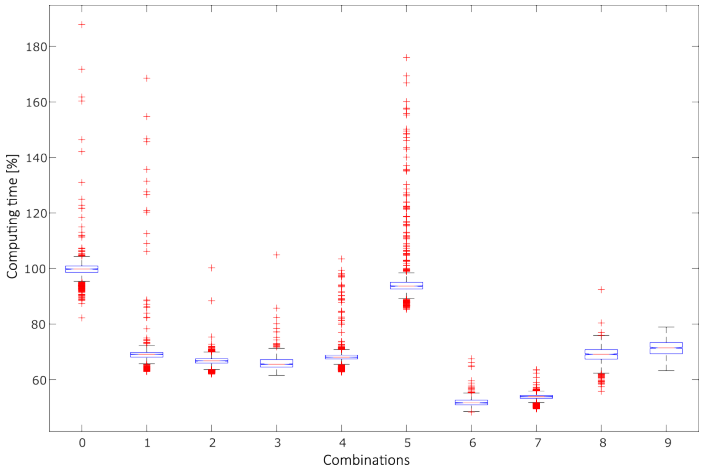

Fig. 5. Box-plots of computing time obtained for each combination of features.

By considering these results and that of accuracy, it emerges that combinations 3 and 4 are the more desirable as they both minimize the computing time, while showing no significant difference in performance with combination-0. In particular, combination-4 appears as the optimal choice due to its consistency in leading to highest accuracy values, as indicated by its low standard deviation (Tab. 3).

4 DISCUSSION

In this study, we investigated how to improve prosthetic control by optimizing the sets of input features to be fed to the classifier. Specifically, we aimed to maximize the prediction accuracy of a pattern recognition algorithm, i.e. ANN, based on the input EMG features, while at the same time minimizing the computational effort, here measured through the computing time required by the machine learning algorithm. We found that optimal performance can be obtained with a subset of 6 features, e.g. combination-3 and combination-4.

This study has some limitations. First, CC does not directly quantify the amount of information carried by each feature. However, it still indicates which sets of features can be considered as redundant and thus which ones can be discarded in favor of quicker computing times. Future development of this study

will explore feature selection by quantifying the information content of each combination of features (e.g., using Shannon Mutual Information [12]). Another limitation lies in the absence of a true prosthetic device and of amputated subjects among the study participants. However, we here aimed at evaluating the classifier performance, which, according to our previous studies, does not change in case of control of a virtual or real prosthetic hand, and also behaves similarly for able bodied and amputated individuals [3], [10].

Future work will also explore whether and how the combination of EMG-derived features affects the performance of different classifiers.

5 CONCLUSIONS

This study indicates that prosthetic control based on pattern recognition algorithms is strongly affected by the choice of input features and that such choice should be guided by taking into account different performance metrics, such as accuracy of prediction and computation effort.

Acknowledgements The authors gracefully acknowledge their colleagues Inna Forsiuk, Simone Tanzarella, Simon Müller-Cleve, Michele Canepa for their support in data collection, and Massimiliano Iacono and Chiara Bartolozzi for useful discussions.

References

1. Cordella, F., Ciancio, A.L., Sacchetti, R., Davalli, A., Cutti, A.G., Guglielmelli, E., Zollo, L.: Literature review on needs of upper limb prosthesis users. Frontiers in neuroscience **10**, 209 (2016), publisher: Frontiers Media SA
2. De Luca, C.J.: The use of surface electromyography in biomechanics. Journal of applied biomechanics **13**(2), 135–163 (1997), publisher: Human Kinetics, Inc.
3. Di Domenico, D., Marinelli, A., Boccardo, N., Semprini, M., Lombardi, L., Canepa, M., Stedman, S., Bellingegni, A.D., Chiappalone, M., Gruppioni, E.: Hannes prosthesis control based on regression machine learning algorithms. pp. 5997–6002. IEEE (2021)
4. Dreiseitl, S., Ohno-Machado, L.: Logistic regression and artificial neural network classification models: a methodology review. Journal of biomedical informatics **35**(5-6), 352–359 (2002), publisher: Elsevier
5. Fougner, A., Stavdahl, Ã., Kyberd, P.J., Losier, Y.G., Parker, P.A.: Control of upper limb prostheses: Terminology and proportional myoelectric control: A review. IEEE Transactions on neural systems and rehabilitation engineering **20**(5), 663–677 (2012), publisher: IEEE
6. Kingma, D.P., Ba, J.: Adam: A method for stochastic optimization. arXiv preprint arXiv:1412.6980 (2014)
7. Lerman, P.: Fitting segmented regression models by grid search. Journal of the Royal Statistical Society Series C: Applied Statistics **29**(1), 77–84 (1980), publisher: Oxford University Press

8. Luu, D.K., Nguyen, A.T., Jiang, M., Xu, J., Drealan, M.W., Cheng, J., Keefer, E.W., Zhao, Q., Yang, Z.: Deep learning-based approaches for decoding motor intent from peripheral nerve signals. Frontiers in Neuroscience **15**, 667907 (2021), publisher: Frontiers Media SA
9. Marinelli, A., Boccardo, N., Tessari, F., Domenico, D.D., Caserta, G., Canepa, M., Gini, G., Barresi, G., Laffranchi, M., Michieli, L.D., Semprini, M.: Active upper limb prostheses: a review on current state and upcoming breakthroughs. Progress in Biomedical Engineering **5**(1), 012001 (Jan 2023). https://doi.org/10.1088/2516-1091/acac57, https://dx.doi.org/10.1088/2516-1091/acac57, publisher: IOP Publishing
10. Marinelli, A., Semprini, M., Canepa, M., Lombardi, L., Stedman, S., Bellingegni, A.D., Chiappalone, M., Laffranchi, M., Gruppioni, E., De Michieli, L.: Performance evaluation of pattern recognition algorithms for upper limb prosthetic applications. pp. 471–476. IEEE (2020)
11. Nguyen, A.T., Drealan, M.W., Luu, D.K., Jiang, M., Xu, J., Cheng, J., Zhao, Q., Keefer, E.W., Yang, Z.: A Portable, Self-Contained Neuroprosthetic Hand with Deep Learning-Based Finger Control. Journal of Neural Engineering **18**(5), 056051 (Oct 2021). https://doi.org/10.1088/1741-2552/ac2a8d, http://arxiv.org/abs/2103.13452, arXiv: 2103.13452
12. Shannon, C.E.: Communication theory of secrecy systems. The Bell system technical journal **28**(4), 656–715 (1949), publisher: Nokia Bell Labs
13. Srivastava, N., Hinton, G., Krizhevsky, A., Sutskever, I., Salakhutdinov, R.: Dropout: a simple way to prevent neural networks from overfitting. The journal of machine learning research **15**(1), 1929–1958 (2014), publisher: JMLR. org
14. Vujaklija, I., Farina, D., Aszmann, O.C.: New developments in prosthetic arm systems. Orthopedic research and reviews pp. 31–39 (2016), publisher: Taylor & Francis